Electronic Supplementary Material (ESI) for Journal of Materials Chemistry A.
This journal is © The Royal Society of Chemistry 2019

Supporting Information

Stable artificial solid electrolyte interphase film for lithium metal anode via metal organic frameworks cemented by Polyvinyl alcohol

Lishuang Fan,[a,b,†] Zhikun Guo,[a,†] Yu Zhang,[a*] Xian Wu, [a] Chenyang Zhao,[a] Xun Sun,[a] Guiye Yang,[a] Yujie Feng,[a] Naiqing Zhang[a,b,*]

[a]State Key Laboratory of Urban Water Resource and Environment, School of Chemistry and Chemical Engineering, Harbin Institute of Technology, China

[b]Academy of Fundamental and Interdisciplinary Sciences, Harbin Institute of Technology, Harbin, 150001, China

[†]L.F. and Z.G. contributed equally to the work.

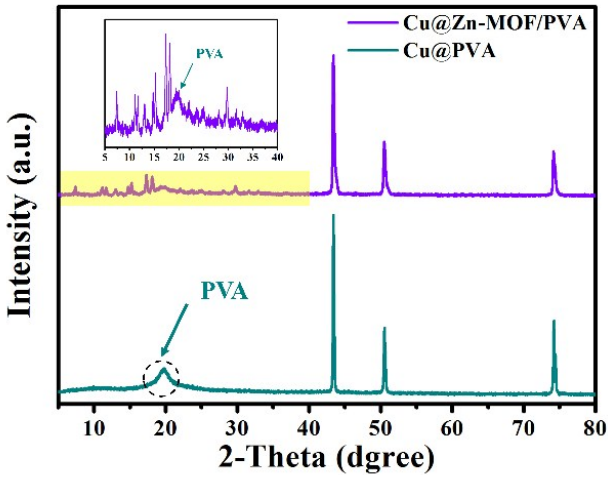

Fig. S1 The XRD patterns of Cu@Zn-MOF/PVA and Cu@PVA

Fig. S2 Contact angles of LiTFSI-DOL/DME electrolyte on the Cu foil、Cu@Zn-MOF and Cu@Zn-MOF/PVA.

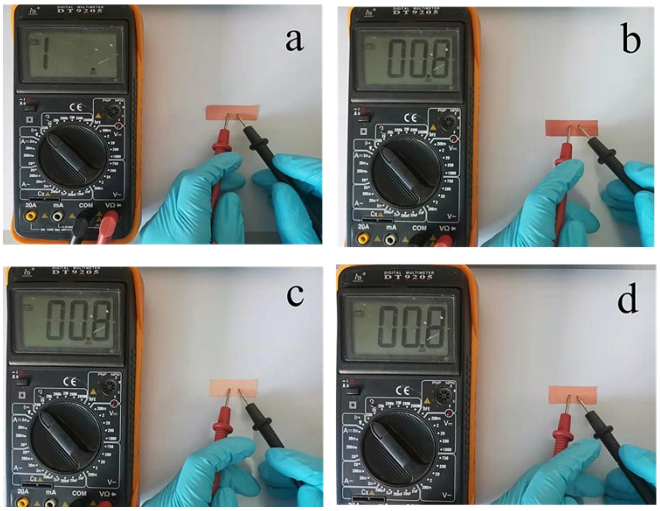

Fig. S3 Apparent resistance of samples (a)Cu@Zn-MOF side (b) Back of Cu@Zn-MOF; (c) Rough (d) Smooth side of Cu foil.

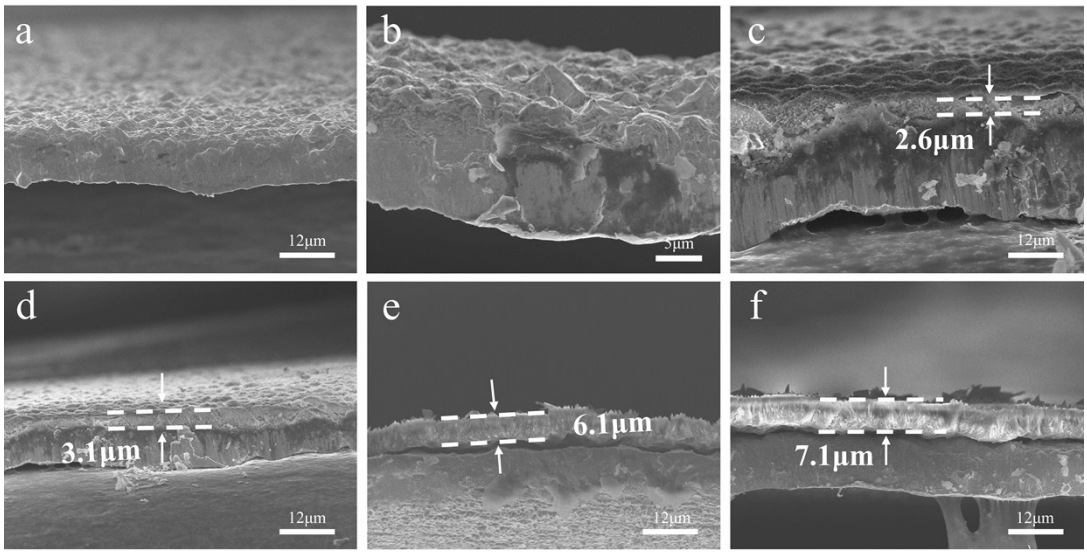

Fig. S4 Cross-sectional SEM images of the Zn-MOF film on Cu foil with different crystallization time (a) 0min, (b) 10 min, (c) 30 min, (d) 1 h, (d) 3 h, (d) 5 h.

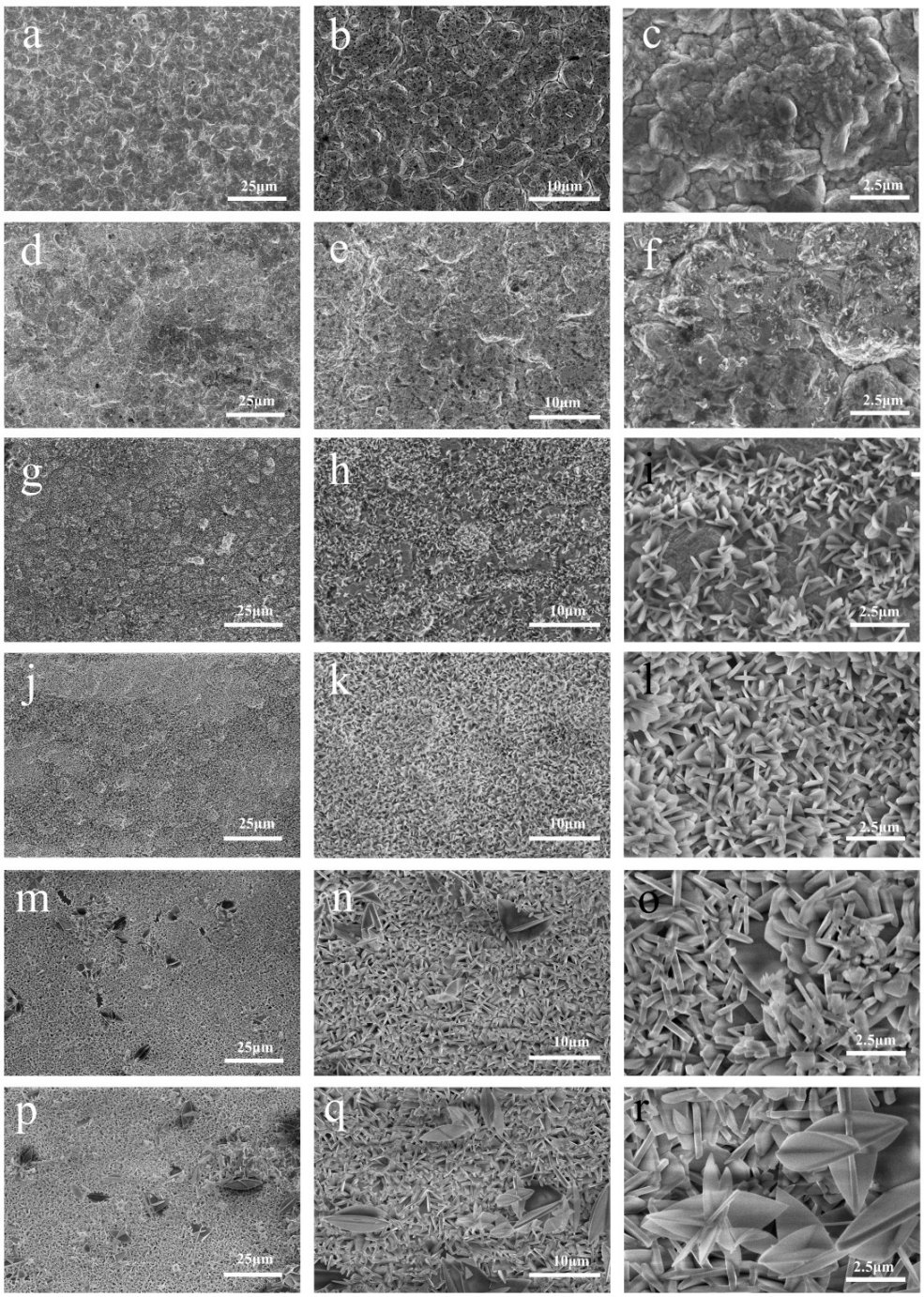

Fig. S5 Top-view SEM images of the Zn-MOF film on Cu foil with different crystallization time (a) (b) (c)0min, (d) (e) (f) 10 min, (g) (h) (i)30 min, (g) (k) (l) 1 h, (m) (n) (o) 3 h, (p) (q) (r) 5 h.

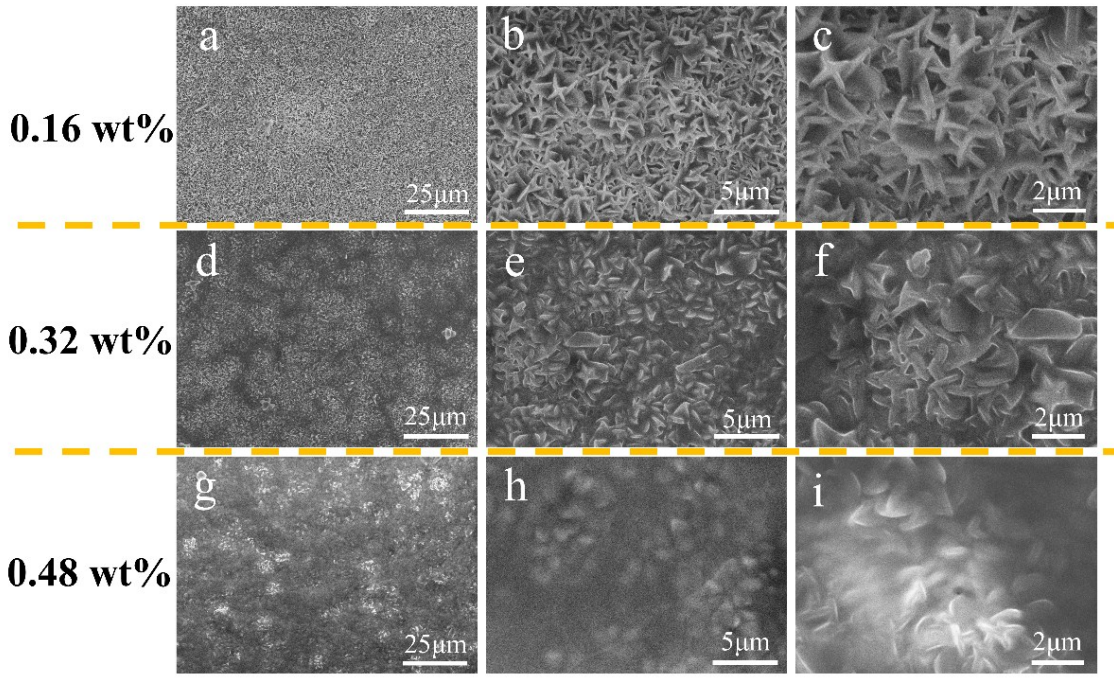

Fig. S6 Top-view SEM images of the Zn-MOF/PVA film on Cu foil with different content of PVA (a) (b) (c) 0.16%, (d) (e) (f) 0.32%, (g) (h) (i) 0.48% .

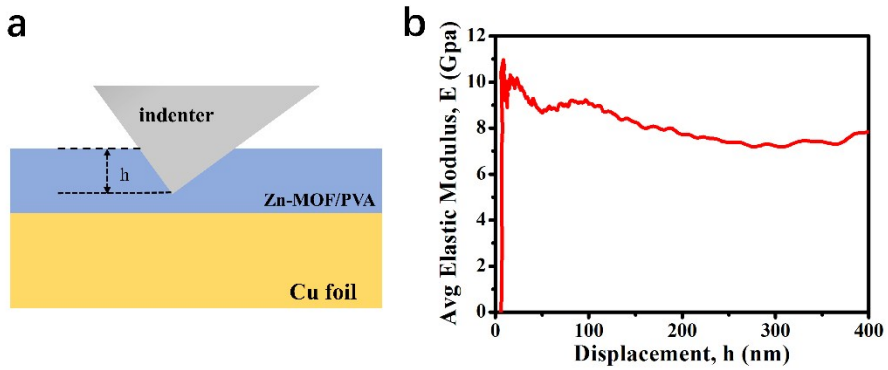

Fig. S7 (a) schematic diagram of nanoindentation test (b) shows the curve of average elastic modulus

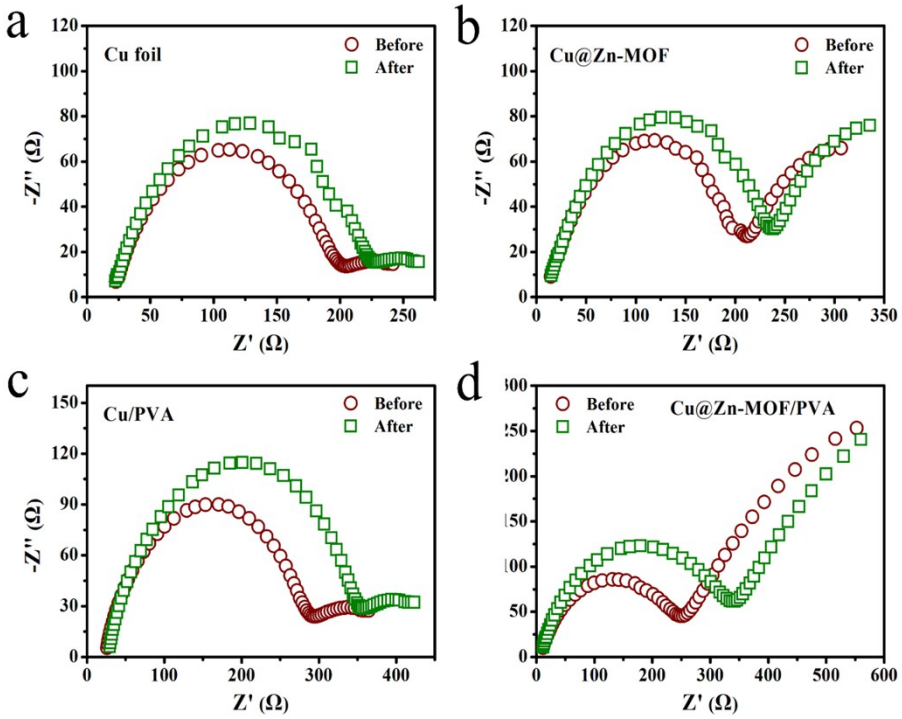

Fig. S8 Impedance change before and after time-current test (a) Cu foil; (b) Cu@Zn-MOF; (c) Cu/PVA; (d) Cu@Zn-MOF/PVA.

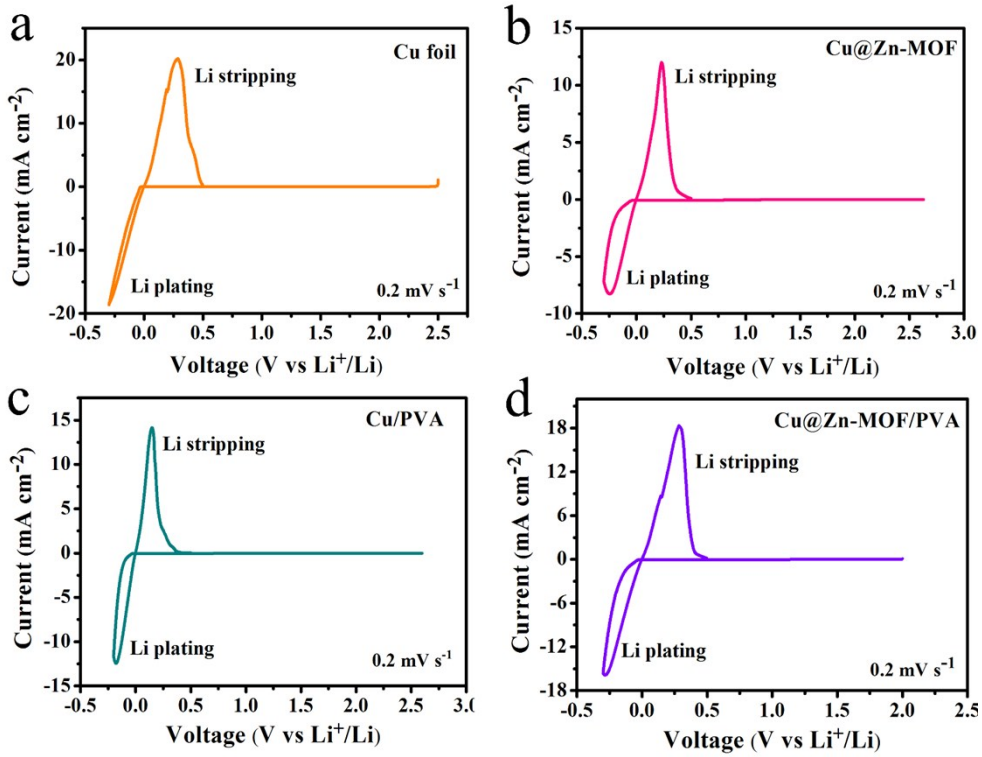

Fig. S9 Cyclic voltammetry curve of artificial SEI film (a) Cu foil; (b) Cu@Zn-MOF; (c) Cu/PVA; (d) Cu@Zn-MOF/PVA.

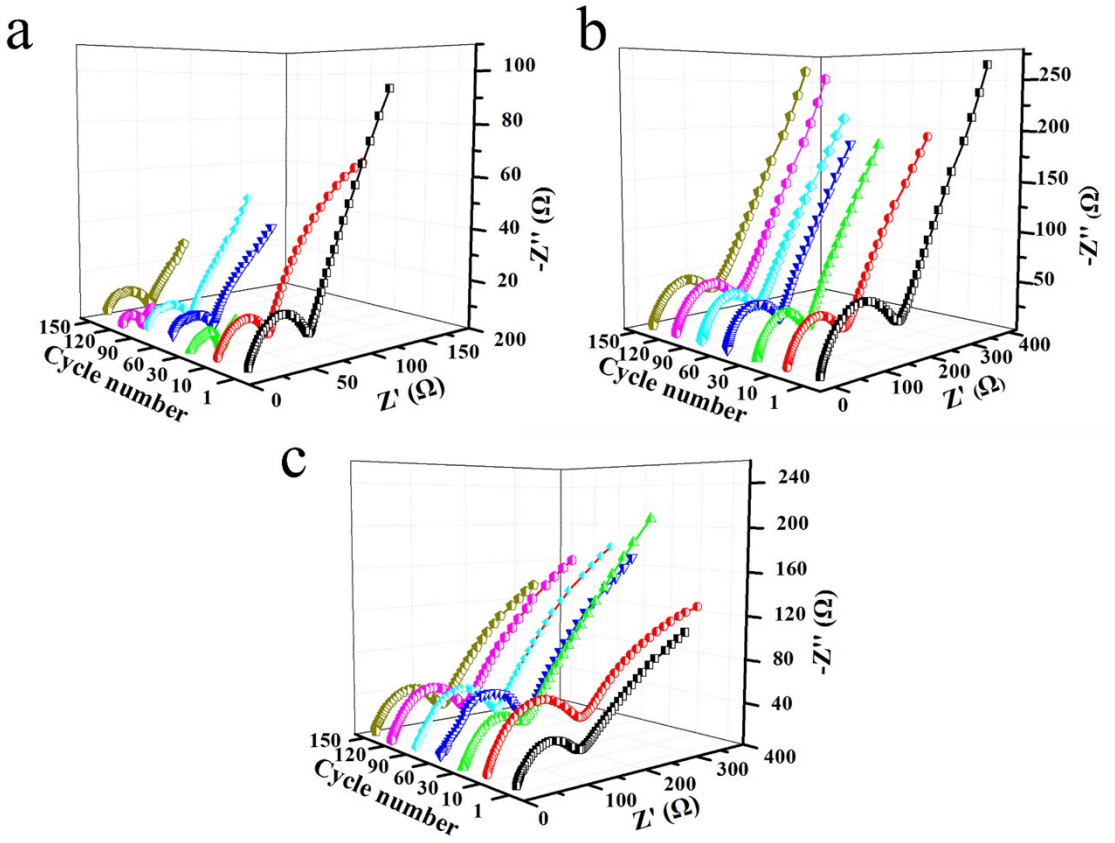

Fig. S10 The electrochemical impedance at different cycle times (a) Cu foil; (b) Cu@Zn-MOF; (c) Cu/PVA;

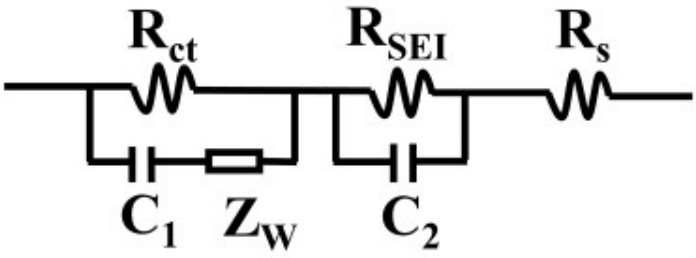

Fig.S11 Impedance equivalent circuit model.

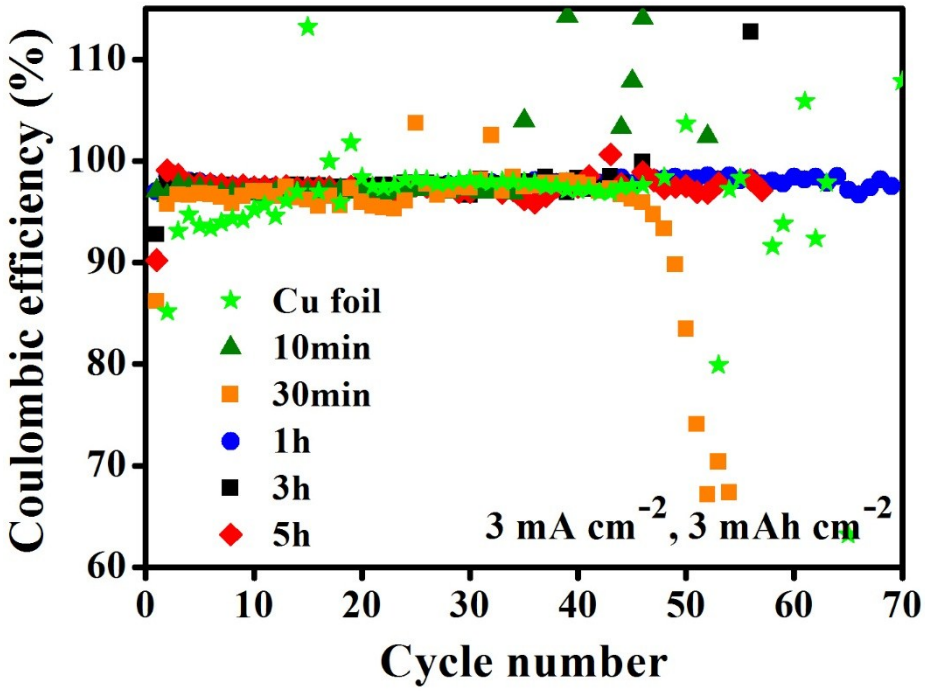

Fig. S12 The coulombic efficiency of the electrode under the protection of Zn-MOF film obtained at different growth times.

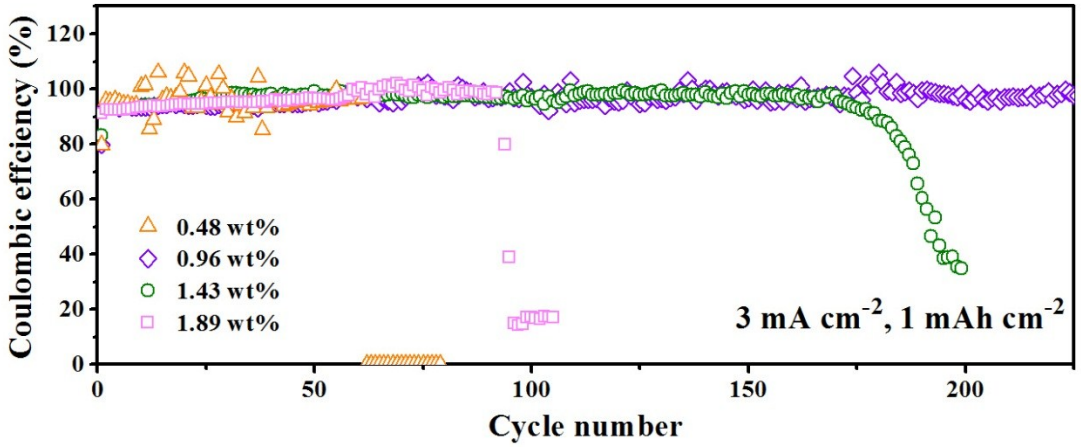

Fig. S13 Coulombic efficiency of PVA with different lithium salt contents.

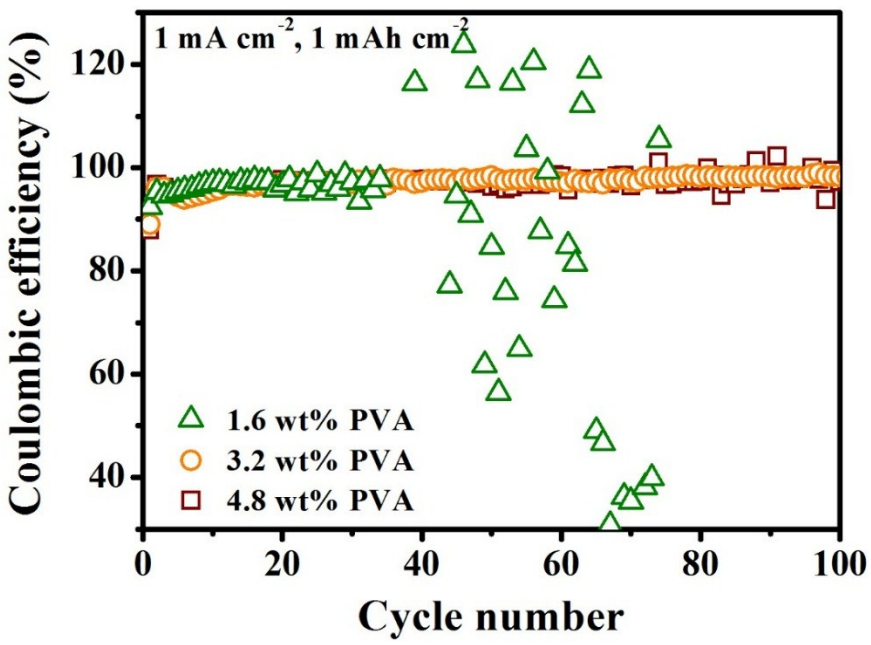

Fig. S14 Coulombic efficiency of Zn-MOF/PVA films with different PVA content.

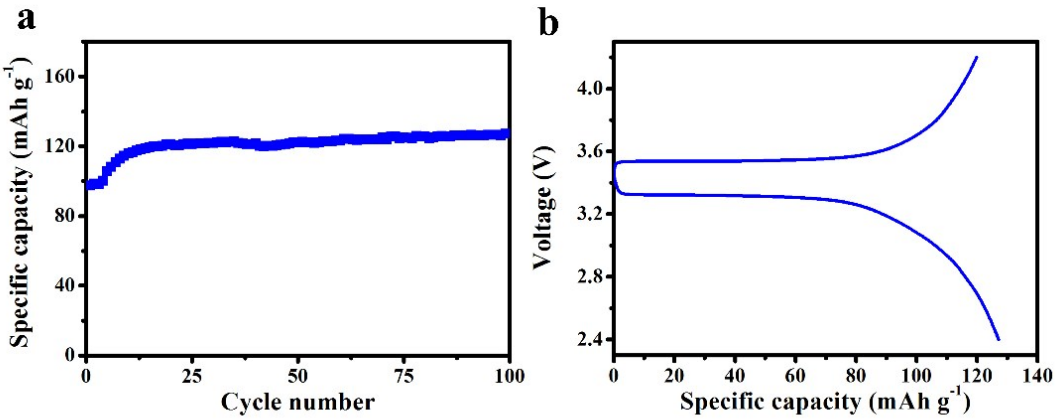

Fig. S15 $LiFePO_4$ and Li foil assembly batteries (a)Cycle performance of the battery at 1C; (b) Charge-discharge voltage curve after 100 cycles.

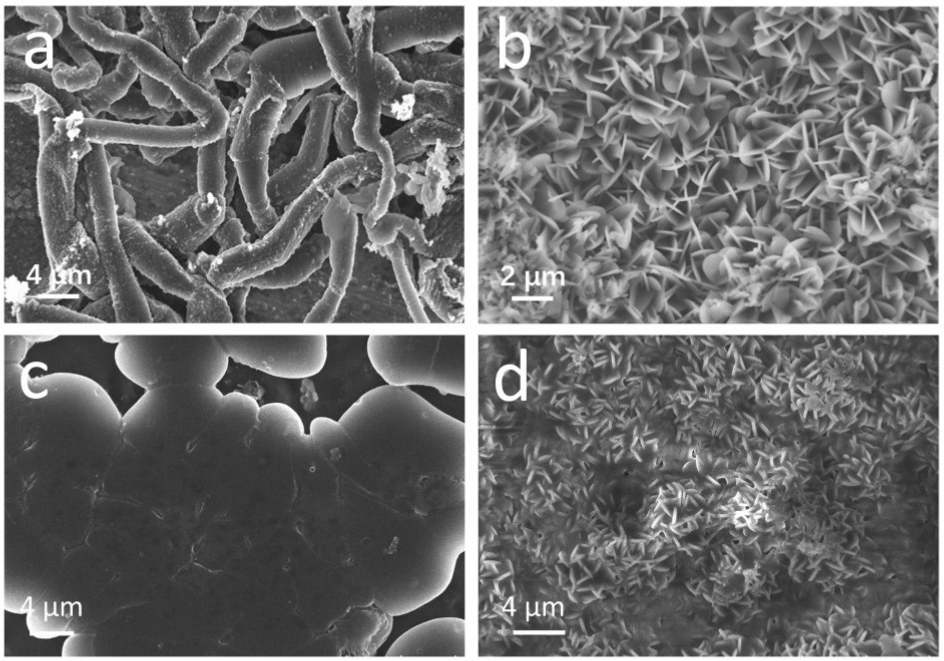

Fig. S16 Top-view SEM images of Li plating/stripping after first cycles on (a) Cu foil, (b) Cu@Zn-MOF,(c) Cu@PVA,(d) Cu@Zn-MOF/PVA with 1 mA cm^{-2}, 1 mAh cm^{-2}.

Table S1. R_s and R_{ct} of Cu foil, Cu@Zn-MOF, Cu@PVA,and Cu@Zn-MOF/PVA

Cycle number		1	10	30	60	90	120	150
Cu foil	R_s/Ω	5.13	4.54	4.35	7.09	6.28	4.99	7.12
	R_{ct}/Ω	14.28	11.48	4.23	6.55	8.43	4.78	8.60
Cu@Zn-MOF	R_s/Ω	3.40	3.56	3.13	3.42	4.09	3.87	4.55
	R_{ct}/Ω	41.87	51.60	33.89	6.75	7.07	39.43	9.13
Cu@ PVA	R_s/Ω	6.22	5.84	7.22	10.95	8.49	5.78	8.90
	R_{ct}/Ω	15.85	15.30	6.36	14.32	11.06	8.83	9.71
Cu@Zn-MOF/PVA	R_s/Ω	3.78	3.63	3.60	3.69	3.72	3.79	3.74
	R_{ct}/Ω	27.45	27.60	29.27	27.89	26.70	26.76	30.17

Table S2. A brief summary of the reported materials for Li metal anode

Electrode Structures	Current density (mA cm^{-2})	Capacity (mAh cm^{-2})	Coulombic efficiency	Cycle	Reference
2D hexagonal BN	1	1	**97%**	**50**	1
	3	1	**95%**	**50**	
Polyacrylonitrile nanofiber	1	1	**97.9%**	**120**	2
	3	1	**97.4%**	**120**	
SEI coated graphene	0.5	0.5	**97%**	**100**	3
Tubular carbon array	1	2	**98%**	**200**	4
Cu_3N-SBR	1	1	**97.6%**	**150**	5
Cu2O/partially reduced graphene oxide	2	1	**95.6%**	**140**	6
"solid-liquid" Interfacial protective layer	0.5	1	**97.6%**	**120**	7
Double-Layer Nanodiamond	1	2	**98.5%**	**150**	8
Polyacrylonitrile submicron fiber array	1	1	**97.4%**	**250**	9
Carbon nanotube	1	2	**92.4%**	**50**	10
GaInSnZn liquid-metal layer	1	0.5	**97.43%**	**100**	11
Cu-CuO-Ni-10	1	1	**95%**	**250**	12
Zn-MOF/PVA	**1**	**1**	**97.3%**	**400**	**This work**
	3	**1**	**97.7%**	**250**	

References

1. Yan, K.; Lee, H.-W.; Gao, T.; Zheng, G.; Yao, H.; Wang, H.; Lu, Z.; Zhou, Y.; Liang, Z.; Liu, Z.; Chu, S.; Cui, Y., Ultrathin Two-Dimensional Atomic Crystals as Stable Interfacial Layer for Improvement of Lithium Metal Anode. *Nano Letters* **2014,** *14* (10), 6016-6022.

2. Liang, Z.; Zheng, G.; Liu, C.; Liu, N.; Li, W.; Yan, K.; Yao, H.; Hsu, P.-C.; Chu, S.; Cui, Y., Polymer Nanofiber-Guided Uniform Lithium Deposition for Battery Electrodes. *Nano Letters* **2015,** *15* (5), 2910-2916.

3. Cheng, X.-B.; Peng, H.-J.; Huang, J.-Q.; Zhang, R.; Zhao, C.-Z.; Zhang, Q., Dual-Phase Lithium Metal Anode Containing a Polysulfide-Induced Solid Electrolyte Interphase and Nanostructured Graphene Framework for Lithium–Sulfur Batteries. *ACS Nano* **2015,** *9* (6), 6373-6382.

4. Guo, J.; Zhao, S.; Yang, H.; Zhang, F.; Liu, J., Electron regulation enabled selective lithium deposition for stable anodes of lithium-metal batteries. *Journal of Materials Chemistry A* **2019,** *7* (5), 2184-2191.

5. Liu, Y.; Lin, D.; Yuen, P. Y.; Liu, K.; Xie, J.; Dauskardt, R. H.; Cui, Y., An Artificial Solid Electrolyte Interphase with High Li-Ion Conductivity, Mechanical Strength, and Flexibility for Stable Lithium Metal Anodes. *Advanced materials* **2017,** *29* (10), 1605531.

6. Liu, Y.; Zhang, S.; Qin, X.; Kang, F.; Chen, G.; Li, B., In-Plane Highly Dispersed Cu_2O Nanoparticles for Seeded Lithium Deposition. *Nano Letters* **2019,** *19* (7), 4601-4607.

7. Liu, K.; Pei, A.; Lee, H. R.; Kong, B.; Liu, N.; Lin, D.; Liu, Y.; Liu, C.; Hsu, P.-c.; Bao, Z.; Cui, Y., Lithium Metal Anodes with an Adaptive "Solid-Liquid" Interfacial Protective Layer. *Journal of the American Chemical Society* **2017,** *139* (13), 4815-4820.

8. Liu, Y.; Tzeng, Y.-K.; Lin, D.; Pei, A.; Lu, H.; Melosh, N. A.; Shen, Z.-X.; Chu, S.; Cui, Y., An Ultrastrong Double-Layer Nanodiamond Interface for Stable Lithium Metal Anodes. *Joule* **2018,** *2* (8), 1595-1609.

9. Lang, J.; Song, J.; Qi, L.; Luo, Y.; Luo, X.; Wu, H., Uniform Lithium Deposition Induced by Polyacrylonitrile Submicron Fiber Array for Stable Lithium Metal Anode. *ACS applied materials & interfaces* **2017,** *9* (12), 10360-10365.

10. Zhang, R.; Cheng, X.-B.; Zhao, C.-Z.; Peng, H.-J.; Shi, J.-L.; Huang, J.-Q.; Wang, J.; Wei,

F.; Zhang, Q., Conductive Nanostructured Scaffolds Render Low Local Current Density to Inhibit Lithium Dendrite Growth. *Advanced materials* **2016,** *28* (11), 2155-2162.

11. Wei, C.; Fei, H.; An, Y.; Tao, Y.; Feng, J.; Qian, Y., Uniform Li deposition by regulating the initial nucleation barrier via a simple liquid-metal coating for a dendrite-free Li–metal anode. *Journal of Materials Chemistry A* **2019,** *7* (32), 18861-18870.

12. Wu, S.; Zhang, Z.; Lan, M.; Yang, S.; Cheng, J.; Cai, J.; Shen, J.; Zhu, Y.; Zhang, K.; Zhang, W., Lithiophilic Cu-CuO-Ni Hybrid Structure: Advanced Current Collectors Toward Stable Lithium Metal Anodes. *Advanced materials* **2018,** *30* (9), 1705830.